Analysis of Experimental Research of Continuous Detonation of Fuel-Air Mixtures

Fedor A. Bykovskii[1], Sergey A. Zhdan[1]

[1] Lavrentyev Institute of Hydrodynamics SB RAS,
630090, Novosibirsk, Russia

1 Introduction

Application of a thermodynamic detonation cycle in air-breathing engines is of interest for modern jet-driven vehicles. In particular, the development of the scientific basis for detonation engines where the fuel is continuously burned in the detonation wave running across the annular combustor [1] (pattern proposed by academician B. V. Voitsekhovskii [2]) is important. Of interest for practice is continuous spin detonation (CSD) of fuel-air mixtures (FAMs) in flow-type combustors. CSD regimes were first obtained in acetylene-air [3], hydrogen-air [4], and syngas-air [5] FAMs. The structure of transverse detonation waves (TDWs) and the flow in their vicinity, as well as conditions, properties, and domains of CSD existence in these FAMs were considered. Independent experimental validation of CSD in the hydrogen-air FAM was performed in [6, 7] and confirmed the CSD existence. The goal of this work is to find the key parameters responsible for the geometric similarity of CSD by varying the geometric parameters of the annular combustor and to determine the influence of additional injection of air on CSD occurrence and on the values of the specific impulses in hydrogen-air and syngas-air mixtures.

2 Experimental Setup

The study was performed in flow-type axisymmetric annular combustors [1]. The detonation chamber was an axisymmetric annular duct of length L_c = 150÷665 mm, which was formed by the outer wall with a diameter d_c = 306 mm (DC 300) or d_c = 503 mm (DC 500) and the inner cylindrical wall. The distance between the walls (the width of the annular duct) was varied within Δ = 7 ÷ 38 mm. The width of the annular slot for air injection was also varied: δ = 1 ÷ 10 mm. The cross-sectional area of the combustor was determined by the formula $S_c = \pi(d_c - \Delta)\cdot\Delta$, and the cross-sectional area of the annular slot for air injection was determined by the formula $S_\delta = \pi(d_c - \delta)\cdot\delta$. Air was fed from a receiver through an annular manifold and then through the annular slot with a flow rate G_{a1}, and the fuel was fed from the receiver through an annular manifold through injectors [1, 5] with a flow rate G_f. The detonation products escaped into the atmosphere. In some experiments, an additional amount of air with a flow rate G_{a2} was injected into the combustor. In this case, additional air was injected from the side of the inner wall of the combustor at a distance L_{a2} from the end face through an annular slot 3.5 mm wide. The process duration was defined by a control system in the time interval t_D = 0.3 ÷ 0.8 s. The detonation was initiated by burning an aluminum foil strip with energy release of about 5 J at a distance of 150 mm from the fuel injector. The entire process was photographed by a Photron FASTCAM SA1.1 675K-M3 high-speed camera through longitudinal windows in the outer wall of the combustor, and the flow rates of the mixture components during the experiment were determined by the method proposed in [1]. In the case of CSD occurrence, its photographic records were used to

Correspondence to: zhdan@hydro.nsc.ru

determine the time of the emergence of TDWs opposite the window Δt, which allowed us to find unambiguous values of the TDW rotation frequency f and the CSD velocity D as a function of the mean diameter by the formulas

$$f = 1/\Delta t, \qquad D = \pi \cdot \langle d_c \rangle / (n \cdot \Delta t). \qquad (1)$$

Here $\langle d_c \rangle = d_c - \Delta$ is the mean diameter of the annular duct of the combustor and n is the number of TDWs along the combustor circumference. A computer-aided system recorded the signals from the gas pressure sensors: in the receivers (p_{ra} and p_{rf}), in the manifolds (p_{ma} and p_{mf}), at the beginning of the combustor at a distance of 15 mm (p_{c1}), and near the combustor exit (static pressure p_{ex} and total pressure p_{ex0}).

In our experiments, we were able to vary three geometric parameters of the combustor (d_c, δ, and Δ) and three parameters of injection of the FAM components (G_{a1}, G_f, and G_{a2}), i.e., four independent parameters of the problem were varied: g_δ, K_S, ϕ_l, α. Here $g_\delta = G_{a1}/S_\delta$ is the specific flow rate of air through the slot of the main injection system at the combustor entrance, $K_S = S_c/S_\delta$ is the dimensionless coefficient of combustor expansion, $\phi_l = G_f/G_{fst}$ is the fuel-to-air ratio in the region of the main injection of air, and $\alpha = G_{a2}/G_{a1}$ is the dimensionless coefficient of additional injection of air. For example, the specific flow rate of the examined FAMs is determined as a combination of these parameters by the formula $g_\Sigma = g_\delta\ (1 + \phi_l/L_s + \alpha)/K_S$. Here $L_s = G_{a1}/G_{f,st}$ is the stoichiometric coefficient and $G_{f,st}$ is the fuel flow rate corresponding to the stoichiometric ratio with air.

3 Experimental results

CSD regimes in three FAMs have been successfully obtained in flow-type annular cylindrical combustors: C_2H_2+air, H_2+air, and CO/H_2+air (see Table 1).

Table 1. Fuel-air mixtures in which CSD regimes were obtained in flow-type annular cylindrical combustors of various diameters.

FAM	Year	d_c, mm	δ, mm	Δ, mm	L_c, mm	f, kHz	n	Reference
C_2H_2+air	2005	306	1-10	23	665	0.9–1.7	1	[3]
H_2+air	2006	306	1-10	16.5-38	310-665	1.15–4.76	1-3	[4]
H_2+air	2011	95;150	0.5-2	5-10	≈ 200	2.76 – 5	1	[6]
CO/H_2+air	2013	306	3	16.5	570	1.41 – 3.0	1-2	[5]

Effect of the air injection slot width. The effect of the parameter δ was studied in experiments in the DC 300 combustor having the sizes L_c = 665 mm and Δ = 23 mm with hydrogen used as a fuel (injector F2 [1]). In these experiments, the width of the annular slot for air injection δ and, hence, the dimensionless geometric parameter K_S were varied by a factor of 10. The generalizing dependences of the TDW rotation frequency f on the specific flow rate of air through the annular slot $g_\delta = G_a/S_\delta$ for the H_2-air mixture with variations of the parameter δ are shown in Fig. 1.

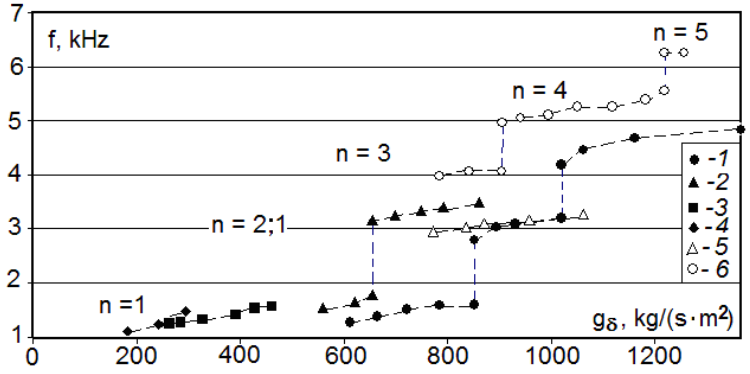

Figure 1. TDW frequency f (kHz) versus the specific flow rate of air through the annular slot g_δ : H_2 - air (injector F2), δ (mm): 2 (1), 3 (2), 6 (3), 10 (4), 3.17 (5) [7], and 2 (6) ($G_{a2} > 0$, $\alpha = 1.1 \rightarrow 0.92$, $L_{a2} = 270$ mm).

For the H_2-air mixture in the examined range of input parameters, we obtained the CSD regime with the TDW rotation frequency in the interval f = (1.15 ÷ 4.76) kHz (see Fig. 1). As the slot width δ increases, the domain of the CSD beginning in terms of the specific flow rate g_δ monotonically decreases. At δ = 1 mm, we have $g_{\delta,\min}$ = 1872 kg/(s·m^2) (not shown in Fig. 1); at δ = 10 mm, we have $g_{\delta,\min}$ = 175 kg/(s·m^2). At a fixed value of the slot width δ, an increase in the parameter g_δ leads to an increase in the TDW rotation frequency. The jumps in the frequency curve correspond to the changes in the number of TDWs that can be accommodated over the combustor perimeter. At δ = 2 mm (curve 1), the one-wave CSD regime emerges at $g_\delta = g_{\delta,\min}$ = 613 kg/(s·m^2), and the TDW rotation frequency is f = 1.27 kHz. As g_δ increases in the interval 613 kg/(s·m^2) < g_δ < 853 kg/(s·m^2), the TDW rotation frequency monotonically increases up to 1.6 kHz. At g_δ = 853 kg/(s·m^2), flow reconstruction occurs in the combustor and a two-wave (n = 2) CSD regime is formed; as a result, the frequency jumps up to f = 2.78 kHz. In the range 853 kg/(s·m^2) < g_δ < 1021 kg/(s·m^2), the TDW rotation frequency increases up to f = 3.2 kHz. At g_δ = 1021 kg/(s·m^2), another flow reconstruction occurs, a three-wave (n = 3) CSD regime is formed, and the frequency jumps up to f = 4.17 kHz and subsequently increases with increasing g_δ. Because of the engineering constraints of the experimental setup in terms of the maximum flow rates of air G_a and fuel G_f, we managed to obtain two wave (n = 2) CSD regimes at δ = 1 mm and 3 mm (curve 2) with increasing specific flow rate of air g_δ; at δ = 6 mm (curve 3) and 10 mm (curve 4), only one-wave (n = 1) CSD regimes could be obtained. For comparison, Fig. 1 also shows the experimental data for the one-wave CSD regime [7] (curve 5), which were obtained for the hydrogen-air FAM in a combustor having a diameter d_c = 152 mm and equipped by an annular slot for air injection with a width δ = 3.17 mm and by a fuel injector with 80 orifices, each 2.54 mm in diameter. It is seen that the data [7] correlate well with our experimental data at δ = 2 mm (curve 1). It was impossible to perform direct comparisons with the data [6] because the authors did not give the flow rates of the H_2-air FAM components used in their experiments.

Thus, at a fixed value of δ, there exists a minimum specific flow rate of air $g_{\delta,\min}(\delta)$ at which a one-wave (n = 1) CSD regime is formed. As the value of g_δ increases, the CSD evolves in accordance with the following sequence: (n = 1) → (n = 2) → (n = 3) → etc. The data of Fig. 1, in particular, allow us to estimate the minimum combustor diameter $d_{c,\min}$ whose value depends on the specific flow rate of air g_δ, geometry of the injector orifices, and degree of combustor expansion. For example, at δ = 2 mm (K_s = 10.71) we obtain the following estimates for $d_{c,\min}$ for the case where the injector F2 is used: $d_{c,\min}$ ≈ 300 mm at $g_{\delta,\min}$ ≥ 613 kg/(s·m^2), $d_{c,\min}$ ≈ 150 mm at $g_{\delta,\min}$ ≥ 853 kg/(s·m^2), and $d_{c,\min}$ ≈ 100 mm at $g_{\delta,\min}$ ≥ 1021 kg/(s·m^2). These estimates of $d_{c,\min}$ obtained on the basis of our experimental data in the DC 300 combustor are consistent with the data [6, 7].

Effect of the combustor diameter. If the parameters g_δ, K_s, and ϕ_l are fixed and the quality of FAM mixing is identical, an increase in the combustor diameter d_c by a factor of 2, 3, etc. with respect to the minimum diameter $d_{c,\min}$ leads to a corresponding increase in the number of TDWs by the same factor. Obviously, a necessary condition of CSD obtaining in TDWs is $d_c > d_{c,\min}$. To check the geometric similarity of the CSD regimes with increasing combustor diameter d_c, we performed special experiments in a flow-type annular cylindrical combustor with an outer diameter d_c = 503 mm, δ = 3.5 mm, Δ = 18 mm, and combustor length L_c = 540 mm. The photographic records of the CSD regime with the syngas having the composition CO + 3H_2 being used as a fuel are shown in Fig. 2.

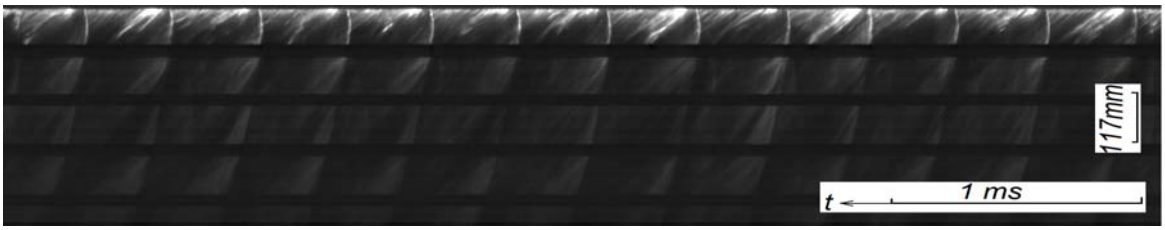

Figure 2. Fragment of typical photographic records of CSD of the CO + 3H_2 + air mixture: d_c = 503 mm, L_c = 540 mm, g_δ = 850 kg/(s·m^2), K_S = 5.0, ϕ_l = 1.42; f = 2.7 kHz, D = 1.43 km/s, and n = 3.

The effect of geometric similarity of the CSD for the CO + $3H_2$ + air mixture is demonstrated in Fig. 3, which shows the TDW rotation frequency f as a function of the specific flow rate of air g_δ in combustors with two different diameters: d_{c1} = 306 mm and d_{c2} = 503 mm.

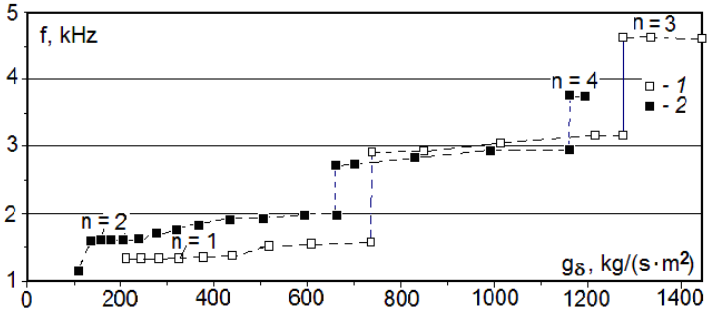

Figure 3. TDW rotation frequency f (kHz) versus the specific flow rate of air through the annular slot g_δ kg/(s·m^2) for the CO + $3H_2$ + air mixture: 1 - d_{c1} = 306 mm (K_S = 5.25); 2 - d_{c2} = 503 mm (K_S = 5.0).

As the specific flow rate of air g_δ increases, the TDW rotation frequency monotonically increases in the intervals f = 1.32 ÷ 4.62 kHz at d_{c1} = 306 mm and f = 1.14 ÷ 3.77 kHz at d_{c2} = 503 mm. The jumps of the frequency f correspond to the instants of the transition from the n-wave CSD regime to the (n+1)-wave regime. The minimum number of waves is one in the combustor with d_{c1} = 306 mm and two in the combustor with d_{c2} = 503 mm. In the range g_δ = 750÷1150 kg/(s·m^2), the TDW rotation frequency and, hence, the CSD velocity remain approximately unchanged, while the number of wave is proportional to the combustor diameter $d_{c2}/d_{c1} \approx n_2/n_1 = 3/2$. Thus, the geometric similarity of the CSD is observed.

In the examined syngas-air mixtures, we measured the detonation front height h, which depends on the composition of the mixture, the number of TDWs, and the domain of the mixture with respect to the limits in terms of ϕ and g_Σ. At n = 2, the value of h was found to change in the interval h = 12 – 15 cm. Smaller values of h corresponded to larger fractions of hydrogen in the combustible mixture. At n = 1 and near the stoichiometric composition, we had h = 18 – 24 cm.

Specific impulses. Injection of an additional amount of air ($G_{a2} > 0$) into the flow is equivalent to constriction of the free cross-sectional area of the stream tubes. Let us determine the effect of air addition to the CSD products on the specific impulse of the combustor. The thrust force is determined by the formula $F = \int [p + \rho u^2 - p_a] dS = (p_{ex0} - p_a) \cdot S_c$. Here ρ is the density, u is the velocity, p_a is the counterpressure, and dS is the area of the elementary stream tube. Measuring the stagnation pressure of the CSD products p_{ex0} at the combustor exit (exhaustion into the atmosphere), we can determine the thrust force F and specific impulse as a function of the fuel flow rate: $I_{sp} = (p_{ex0} - p_a) \cdot S_c/(G_f \cdot g)$. Here g = 9.81 m/s^2 is the free-fall acceleration. Figure shows the specific impulses $I_{sp,f}$ for the CSD in the H_2–air and CO + $3H_2$ – air FAMs versus the total pressure p_{ex0} for the case of exhaustion of the CSD products into the atmosphere.

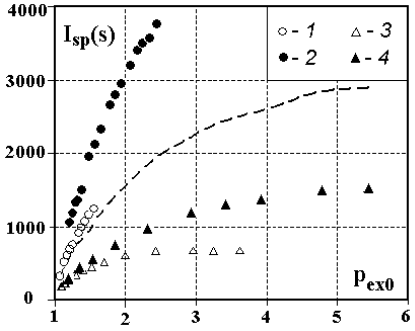

Figure 4. Specific impulses $I_{sp,}$(s) during the CSD versus the total pressure at the combustor exit p_{ex0} (atm): a) H_2-air (K_s = 10.7) [8]: G_{a2} = 0 (1), $G_{a2} > 0$ (2), α = 1.1 → 0.92; b) CO + $3H_2$ – air (K_s = 5.25): G_{a2} = 0 (3), $G_{a2} >$ 0 (4), α = 1.02 → 0.

As the total pressure p_{ex0} increases, the specific impulses I_{sp} for the examined FAMs increase monotonically both with additional injection of air ($\alpha > 0$) and without it ($\alpha = 0$). At the maximum values of p_{ex0} obtained in this series of experiments, the specific impulses I_{sp} for the H_2–air mixture have not yet reached the extreme value. At $G_{a2} = 0$ (curves 1 and 3) and the greatest values of p_{ex0}, the values of the specific impulses for the H_2–air mixture are almost twice the values of the specific impulses for the $CO + 3H_2$ mixture. At $G_{a2} > 0$, the specific impulses in all mixtures are seen to increase. Thus, for the H_2–air mixture at $\alpha > 0$ (curve 2) and $p_{ex0} = 1.5$ atm ($\alpha = 0.98$), we have $I_{sp} \approx$ 1960 s, which is greater than the corresponding value at $\alpha = 0$ (curve 1) almost by a factor of 1.6. At the greatest value of $p_{ex0} = 2.4$ atm obtained in these experiments ($\alpha = 1.1$), we have $I_{sp} \approx 3780$ s for the H_2–air mixture. For the $CO + 3H_2$ – air mixture ($\alpha > 0$, curve 4), we have $I_{sp} \approx 1330$ s at $p_{ex0} = 3.6$ atm ($\alpha = 0.57$), which is almost twice higher than the corresponding value at $\alpha = 0$ (curve 3); at the maximum experimental value $p_{ex0} = 5.4$ atm, we have $I_{sp} \approx 1530$ s. The following comment should be made about the specific impulses I_{spf} for syngas-containing mixtures. In real engines, the syngas will be generated in a special device ahead of the combustpr due to preliminary conversion of the original hydrocarbon fuel. Therefore, rigorously speaking, it is necessary to calculate the specific impulse with respect to the flow rate of the original hydrocarbon fuel rather than with respect to the syngas flow rate. This means that the values of the specific impulses for the $CO + 3H_2$ – air mixture in Fig. 4 (curves 3 and 4) should be increased by a factor of 1.89 to obtain the specific impulses $I_{sp,f0}$ with respect to the flow rate of the original hydrocarbon fuel. These data at $\alpha > 0$ are shown by the dashed curve in Fig. 4. For the $CO + 3H_2$ – air mixture at $p_{ex0} = 5.4$ atm ($\alpha = 1.02$), we have $I_{spf0} \approx 2890$ s. The enhancement factor is 2 for the $CO + 2H_2$ – air mixture and 2.14 for the $CO + H_2$ – air mixture. Thus, we have $I_{sp,f0} = 2600$ s in experiments with the $CO + 2H_2$ fuel at $p_{ex0} = 5.1$ atm ($\alpha = 1.55$) and $I_{sp,f0} =$ 2972 s in experiments with the $CO + H_2$ fuel at $p_{ex0} = 5.09$atm ($\alpha = 1.02$).

Domain of CSD existence. In a flow-type annular combustor with a diameter $d_c = 306$ mm and length $L_c = 500 \div 885$ mm with a fixed geometry of the fuel injectors, we varied the width of the annular slot for air injection δ, the width of the combustor duct Δ, and the specific flow rate of air through the slot g_δ. The experimental data on CSD existence at $\alpha = 0$ allow us to construct the domain of its existence in independent coordinates K_S, ϕ_1, g_δ. These domains of CSD existence in the coordinates (ϕ_1 , g_δ) for two values of the geometric parameter K_S and three FAMs (C_2H_2 – air, H_2 – air, and CO/H_2 – air) are shown in Fig. 5.

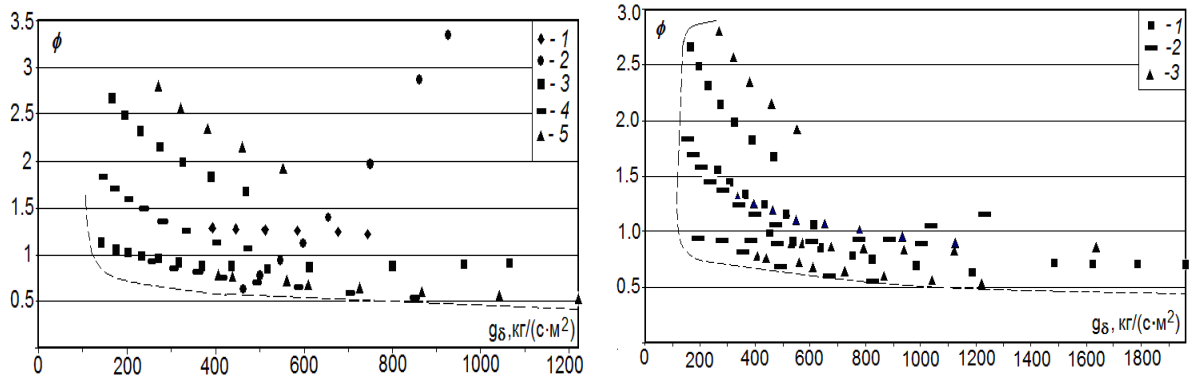

Figure 5. Domain of CSD existence in the coordinates (g_δ, ϕ_1): a) $K_S = 7.16$: C_2H_2 (1), H_2 (2), $CO + H_2$ (3), $CO + 2H_2$ (4), and $CO + 3H_2$ (5); b) $K_S = 5.25$: $CO + H_2$ (1), $CO + 2H_2$ (2), and $CO + 3H_2$ (3).

No detonation regimes are observed below and to the left of the dotted line (usual combustion is observed). The upper limits in terms of the specific flow rate g_δ could not be ensured by the available experimental setup. Nevertheless, we can argue that all CSD regimes bounded from below by the dotted line and by the boundaries of the frame (top right corner) are feasible. At $g_\delta > 600$ kg/(s·m^2), we see the lower limit in terms of the fuel-to-air equivalence ratio: $\phi_1 \approx 0.5$. It weakly decreases with

increasing g_δ. As K_S decreases, the left boundary of the domain of CSD existence expands in terms of the parameter g_δ. As the parameter K_S decreases, the boundary in terms of g_δ is shifted to the left. For example, at $K_S = 2.65$ ($\delta = 6$ mm and $\Delta = 16.5$ mm), it expands for the syngas with the composition $CO+3H_2$ up to $g_\delta = 100$ kg/(s·m^2). It should be noted that the domain of CSD existence in a flow-type combustor (Fig. 5) was constructed for both cold air and cold fuel ($T_0 = 300$ K) escaping from the receiver. Thus, our systematic experiments allowed us to determine the domain of CSD existence for three FAMs (C_2H_2 – air, H_2 – air, and CO/H_2 – air) as a function of the independent parameters g_δ and ϕ_1) for several values of the combustor expansion coefficient K_S.

The analysis of the CSD parameters for three above-mentioned FAMs allows us to argue that it is more difficult to obtain the CSD in syngas-air mixtures than in a more chemically active H_2 – air mixture. It is also definitely found that reduction of the fraction of hydrogen in the syngas composition at identical specific flow rates of the syngas-air mixtures leads to reduction of the TDW velocity and the number of TDWs.

4 Summary

Multi-wave CSD regimes in syngas-air mixtures are obtained for the first time in flow-type annular cylindrical combustors with diameters $d_{c1} = 306$ mm and $d_{c2} = 503$ mm. It is found that the CSD is a high-frequency process with a frequency of 1÷6 kHz; it exists in a wide range of the governing parameters and possesses an effect of scalability. The limits of CSD existence in terms of the fuel-to-air ratio (minimum and maximum values) and the specific rates of the mixture components (minimum values) are determined. The structure of transverse detonation waves and the wave front heights for syngas-air TDWs are close to those previously found by our team for hydrogen-air mixtures. Owing to injection of additional air into the annular combustor, the CSD admits a four-fold decrease in the fuel concentration as compared to the stoichiometric mixture, simultaneously providing a decrease in the temperature of the CSD products and an increase in the specific impulse.

5 Acknowledgement

This work was supported by the Russian Foundation for Basic Research (Grant No. 13-01-00178a) and by the Grant of the President of the Russian Federation (No. NSh 2695. 2014.1).

References

[1] Bykovskii F.A., and Zhdan S.A. (2013) *Continuous spin detonation.* Novosibirsk: Siberian Branch of the Russian Academy of Sciences Publ. 423 p.

[2] Voitsekhovskii B.V. (1959) Steady detonation. *Dokl.. Acad. Sci. USSR.* 129, (6): 1254.

[3] Bykovskii F.A., Zhdan S.A., and Vedernikov E.F. (2005) Spin Detonation of a Fuel–Air Mixture in a Cylindrical Combustor. Dokl. Ross. Akad. Nauk. 400 (3): 338.

[4] Bykovskii F.A., Zhdan S.A., and Vedernikov E.F. (2006) Continuous spin detonation of fuel-air mixtures. *Comb., Expl. Shock Waves*. 42 (4): 463.

[5] Bykovskii F.A., Zhdan S.A., and Vedernikov E.F. (2013) Continuous spin detonation of synthesis gas-air mixtures. *Comb., Expl. Shock Waves*. 49 (4): 435.

[6] Kindracki J., Kobiera A., Wolanski P. et al. (2011) Experimental and numerical study of the rotating detonation engine in hydrogen-air mixtures. *Progress in Propulsion Physics* (2): 555.

[7] Shank J.C. (2012) Development and testing of a rotating detonation engine run on hydrogen and air. //AFIT/GAE/ENY/12-M36. Thesis. 86 p.

[8] Bykovskii F.A., Zhdan S.A., and Vedernikov E.F. (2010) Continuous spin detonation of a hydrogen-air mixture with addition of air into the products and the mixing region. *Comb., Expl. Shock Waves*. 46 (1): 52.